Scattering of π^- Mesons in the Momentum Range 875–1579 MeV/c from a Polarized Proton Target

P. J. Duke, D. P. Jones, M. A. R. Kemp, P. G. Murphy,* J. J. Thresher, and H. H. Atkinson
Rutherford High Energy Laboratory, Chilton, Didcot, Berkshire, England

AND

C. R. Cox and K. S. Heard
Department of Nuclear Physics, Oxford University, Oxford, England

(Received 21 August 1967)

Measurements have been made of the asymmetry in the scattering of π^- mesons by a polarized proton target. Scattered π mesons and recoil protons were detected in arrays of scintillation counters; data were obtained at 16 scattering angles at each of 8 beam momenta between 875 and 1578 MeV/c. Analysis of these data together with earlier differential-cross-section measurements shows that there must exist at least three resonances in this energy region: (i) mass 1920 MeV/c^2, $\Gamma=170$ MeV/c^2, $I=\frac{3}{2}$, $F_{7/2}$; (ii) mass 1682 MeV/c^2, $\Gamma=100$ MeV/c^2, $I=\frac{1}{2}$, $F_{5/2}$; and (iii) mass 1674 MeV/c^2, $\Gamma=100$ MeV/c^2, $I=\frac{1}{2}$, $D_{5/2}$.

I. INTRODUCTION

THE experiment described in this paper is a sequel to the one described earlier,[1] where the results of an experiment on the elastic scattering of positive and negative π mesons by unpolarized protons were reported. The subject of this paper is an experiment on the scattering of negative π mesons from polarized protons, covering the same energy range as Ref. 1. A preliminary report of this work has been published.[2]

It is well known (see Sec. II) that the information obtainable from the scattering of spin-zero mesons by polarized protons is identical with that given by measurements of the polarization of the recoiling protons when the mesons are scattered from unpolarized protons. Fermi[3] pointed out that such measurements would resolve certain ambiguities in the phase-shift interpretation of π-meson–proton scattering results. Since that time several experiments have been reported on recoil proton polarization measurements in this region of energy.[4,5] This type of experiment suffers from two defects. The first is that the recoiling protons must have at least 80-MeV kinetic energy for it to be practical to measure their polarization by scattering from a second target; this limits the range of meson scattering angles accessible to the experiment. The second drawback is that an enormous number of double scattering events is necessary to obtain accurate results at several angles—even at a single energy. Since useful interpretation can only be made when the energy dependence of the angular distribution of the polarization is known, it is obvious that double scattering is a most laborious method for studying proton polarization effects.

The development of targets containing protons with a high degree of polarization[6,7] has made the single scattering experiments feasible. It is possible to arrange the experiment so that the events recorded are predominantly due to the free polarized protons rather than the unpolarized protons bound in the nuclei of the target material [$La_2Mn_3(NO_3)_{12}24H_2O$], even though this compound contains 15 bound protons for each free proton. The experiment consists of a measurement of the dependence of the scattering cross section on the sign of the proton polarization in the direction normal to the scattering plane. It is this type of experiment which is reported here.

II. THEORY OF PION-NUCLEON SCATTERING

A. Isotopic Spin

Assuming charge independence, any pion-nucleon scattering amplitude can be expressed in terms of the scattering amplitudes $M^{(1/2)}$ and $M^{(3/2)}$ for the pure isotopic spin states with $I=\frac{1}{2}$ and $\frac{3}{2}$, respectively. Some of these expressions are given in Table I. Amplitudes for scattering off neutrons can be obtained by applying charge symmetry. From Table I expressions can be derived for total cross sections and differential elastic

Table I. Pion-proton scattering amplitudes in terms of isotopic spin eigenamplitudes. Pion-neutron amplitudes can be obtained by using charge symmetry.

Scattering state	Amplitude
$\pi^+p\rightarrow\pi^+p$	$M^{(3/2)}$
$\pi^-p\rightarrow\pi^-p$	$\frac{1}{3}M^{(3/2)}+\frac{2}{3}M^{(1/2)}$
$\pi^-p\rightarrow\pi^0n$	$\frac{1}{3}\sqrt{2}(M^{(3/2)}-M^{(1/2)})$

* Present address: The Physical Laboratories, The University, Manchester 13, England.

[1] P. J. Duke, D. P. Jones, M. A. R. Kemp, P. G. Murphy, J. D. Prentice, and J. J. Thresher, Phys. Rev. **149**, 1077 (1966).

[2] P. J. Duke, D. P. Jones, M. A. R. Kemp, P. G. Murphy, J. D. Prentice, J. J. Thresher, H. H. Atkinson, C. R. Cox, and K. S. Heard, Phys. Rev. Letters **15**, 468 (1965).

[3] E. Fermi, Phys. Rev. **91**, 947 (1953).

[4] E. F. Beall, B. Cork, C. M. P. Johnson, L. J. Koester, Jr., P. G. Murphy, and W. A. Wenzel, Phys. Rev. **126**, 1554 (1962).

[5] R. D. Eandi, T. J. Devlin, R. W. Kenney, P. G. McManigal, and B. J. Moyer, Phys. Rev. **136**, 536 (1964).

[6] A. Abragam, M. Borghini, P. Catillon, J. Coustham, P. Roubeau, and J. Thirion, Phys. Letters **2**, 310 (1962).

[7] O. Chamberlain, C. D. Jeffries, C. H. Schultz, G. Shapiro, and L. Van Rossum, Phys. Letters **7**, 293 (1963).

TABLE II. Coefficients $c_{n\alpha\beta}$ in the expansion $d\sigma/d\Omega=\sum_n \sum_{\alpha\geq\beta} c_{n\alpha\beta}\,\mathrm{Re}(A_\alpha^{(-)*}A_\beta^{(-)})P_n(\cos\theta^*)$.

$A_\alpha A_\beta$	$c_{0\alpha\beta}$	$c_{2\alpha\beta}$	$c_{4\alpha\beta}$	$c_{6\alpha\beta}$	$c_{8\alpha\beta}$	$A_\alpha A_\beta$	$c_{1\alpha\beta}$	$c_{3\alpha\beta}$	$c_{5\alpha\beta}$	$c_{7\alpha\beta}$
$S_{1/2}S_{1/2}$	1					$P_{1/2}S_{1/2}$	2			
$P_{1/2}P_{1/2}$	1					$P_{3/2}S_{1/2}$	4			
$P_{3/2}P_{1/2}$		4				$D_{3/2}P_{1/2}$	4			
$P_{3/2}P_{3/2}$	2	2				$D_{3/2}P_{3/2}$	0.80	7.20		
$D_{3/2}S_{1/2}$		4				$D_{5/2}P_{1/2}$		6		
$D_{3/2}D_{3/2}$	2	2				$D_{5/2}P_{3/2}$	7.20	4.80		
$D_{5/2}S_{1/2}$		6				$F_{5/2}S_{1/2}$		6		
$D_{5/2}D_{3/2}$		1.71	10.29			$F_{5/2}D_{3/2}$	7.20	4.80		
$D_{5/2}D_{5/2}$	3	3.43	2.57			$F_{5/2}D_{5/2}$	0.51	3.20	14.29	
$F_{5/2}P_{1/2}$		6				$F_{7/2}S_{1/2}$		8		
$F_{5/2}P_{3/2}$		1.71	10.29			$F_{7/2}D_{3/2}$		2.67	13.33	
$F_{5/2}F_{5/2}$	3	3.43	2.57			$F_{7/2}D_{5/2}$	10.29	8	5.71	
$F_{7/2}P_{1/2}$			8			$G_{7/2}P_{1/2}$		8		
$F_{7/2}P_{3/2}$		10.29	5.71			$G_{7/2}P_{3/2}$		2.67	13.33	
$F_{7/2}F_{5/2}$		1.14	4.68	18.18		$G_{7/2}F_{5/2}$	10.29	8	5.71	
$F_{7/2}F_{7/2}$	4	4.76	4.21	3.03		$G_{7/2}G_{7/2}$	0.38	2.18	6.59	22.84
$G_{7/2}S_{1/2}$			8			$G_{9/2}P_{1/2}$			10	
$G_{7/2}D_{3/2}$		10.29	5.71			$G_{9/2}P_{3/2}$		13.33	6.67	
$G_{7/2}D_{5/2}$		1.14	4.68	18.18		$G_{9/2}F_{5/2}$		1.82	6.15	22.03
$G_{7/2}G_{7/2}$	4	4.76	4.21	3.03		$G_{9/2}F_{7/2}$	13.33	10.91	9.23	6.53
$G_{9/2}S_{1/2}$			10							
$G_{9/2}D_{3/2}$			3.64	16.36						
$G_{9/2}D_{5/2}$		14.29	9.35	6.36						
$D_{9/2}G_{7/2}$		0.87	3.24	8.48	27.41					
$G_{9/2}G_{9/2}$	5	6.06	5.66	4.85	3.43					

cross sections. For example,

$$\sigma_{\mathrm{tot}}(\pi^+p)=\sigma_{\mathrm{tot}}{}^{(3/2)}, \tag{1}$$

$$\sigma_{\mathrm{tot}}(\pi^-p)=\tfrac{1}{3}\sigma_{\mathrm{tot}}{}^{(3/2)}+\tfrac{2}{3}\sigma_{\mathrm{tot}}{}^{(1/2)}, \tag{2}$$

$$(d\sigma/d\Omega)(\pi^+p\rightarrow\pi^+p)=|M^{(3/2)}|^2, \tag{3}$$

$$(d\sigma/d\Omega)(\pi^-p\rightarrow\pi^-p)=\tfrac{1}{9}|M^{(3/2)}|^2+(4/9)|M^{(1/2)}|^2+(4/9)\,\mathrm{Re}(M^{(3/2)*}M^{(1/2)}), \tag{4}$$

$$(d\sigma/d\Omega)(\pi^-p\rightarrow\pi^0n)=(2/9)|M^{(3/2)}|^2+(2/9)|M^{(1/2)}|^2-(4/9)\,\mathrm{Re}(M^{(3/2)*}M^{(1/2)}). \tag{5}$$

From (4) we see that elastic scattering of π^- by protons is dominated by scattering in the $I=\frac{1}{2}$ state and interference between the $I=\frac{1}{2}$ and $I=\frac{3}{2}$ states.

In order to describe the dependence on the proton spin state the amplitudes M must have two components. Each M can then be expressed as

$$M=f+ig\boldsymbol{\sigma}\cdot\hat{n}\sin\theta^*, \tag{6}$$

where f and g (each with one component) are, respectively, the non-spin-flip and spin-flip amplitudes.[8] f and g decompose as before; e.g., for π^-p scattering $f^{(-)}=\frac{2}{3}f^{(1/2)}+\frac{1}{3}f^{(3/2)}$, $g^{(-)}=\frac{2}{3}g^{(1/2)}+\frac{1}{3}g^{(3/2)}$. $\hat{n}$ is a unit vector in the direction of $\mathbf{k}_i\times\mathbf{k}_f$, where $\mathbf{k}_i$ and $\mathbf{k}_f$ are the initial and final momenta (of either particle), in the center-of-mass (c.m.) system.

All measurable quantities can be expressed in terms of the f and the g. For example, the differential cross section for scattering from an unpolarized target is

$$d\sigma/d\Omega=|f|^2+|g|^2\sin^2\theta. \tag{7}$$

If P_p is the polarization of the recoil proton from an unpolarized target in the direction $\hat{n}$, then

$$P_p d\sigma/d\Omega=2\sin\theta^*\,\mathrm{Im}(fg^*), \tag{8}$$

where θ^* is the scattering angle in the c.m. system. The left-right asymmetry ϵ in the scattering from a proton target polarized in the direction $\hat{n}$, when the target polarization is P_T is given by

$$(\epsilon/P_T)d\sigma/d\Omega=2\sin\theta^*\,\mathrm{Im}(fg^*). \tag{9}$$

Thus ϵ and P_p give the same information about f and g. It is also possible to measure the components of the polarization of the recoil proton from targets polarized in various other directions. These measurements can be expressed in terms of parameters D, A, R, etc., (analogous to the parameters of nucleon-nucleon scattering) which in turn are related to f and g. In the case of scattering of a spin-0 particle by a spin-$\frac{1}{2}$ particle only one of these parameters is independent, given P_p or ϵ and $d\sigma/d\Omega$. All these parameters are defined by Roper and Wright.[9]

B. Partial-Wave Expansion

The $f^{(I)}(\theta^*)$ and $g^{(I)}(\theta^*)$ can be expanded in series of partial waves:

$$f^{(I)}(\theta^*)=\sum_{l=0}^{\infty}[(l+1)A_{l+}{}^{(I)}+lA_{l-}{}^{(I)}]P_l(\cos\theta^*), \tag{10}$$

$$g^{(I)}(\theta^*)=\sum_{l=1}^{\infty}(A_{l+}{}^{(I)}-A_{l-}{}^{(I)})P_l'(\cos\theta^*), \tag{11}$$

where the partial waves $A_l{}^{\pm(I)}$ correspond to $J=l\pm\frac{1}{2}$. The unitarity condition permits each $A_l{}^{\pm(I)}$ to be

[8] The factor $\sin\theta^*$ is frequently absorbed into g by definition; this is done, for example, in Ref. 1.

[9] L. David Roper and Robert M. Wright, Lawrence Radiation Laboratory Report No. UCRL 7846 (unpublished).

TABLE III. Coefficients $d_{n\alpha\beta}$ in the expansion $(\epsilon/P_T)d\sigma/d\Omega=\sum_n \sum_{\alpha>\beta} d_{n\alpha\beta}\,\mathrm{Im}(A_\alpha^{(-)*}A_\beta^{(-)})\,\sin\theta^* P_n(\cos\theta^*)$.

$A_\alpha A_\beta$	$d_{0\alpha\beta}$	$d_{2\alpha\beta}$	$d_{4\alpha\beta}$	$d_{6\alpha\beta}$	$A_\alpha A_\beta$	$d_{1\alpha\beta}$	$d_{3\alpha\beta}$	$d_{5\alpha\beta}$	$d_{7\alpha\beta}$
$P_{1/2}S_{1/2}$	−2				$P_{3/2}P_{1/2}$	6			
$P_{3/2}S_{1/2}$	2				$D_{3/2}S_{1/2}$	−6			
$D_{3/2}P_{1/2}$	−2				$D_{5/2}S_{1/2}$	6			
$D_{3/2}P_{3/2}$	−6	−16			$D_{5/2}D_{3/2}$	12	18		
$D_{5/2}P_{1/2}$	2	10			$F_{5/2}P_{1/2}$	−6			
$D_{5/2}P_{3/2}$	4	2			$F_{5/2}P_{3/2}$	−12	−18		
$F_{5/2}S_{1/2}$	−2	−10			$F_{7/2}P_{1/2}$	6	14		
$F_{5/2}D_{3/2}$	−4	−2			$F_{7/2}P_{3/2}$	12	4		
$F_{5/2}D_{5/2}$	−6	−22.28	−25.71		$F_{7/2}F_{5/2}$	18	32.67	33.33	
$F_{7/2}S_{1/2}$	2	10			$G_{7/2}S_{1/2}$	−6	−14		
$F_{7/2}D_{3/2}$	4	20	24		$G_{7/2}D_{3/2}$	−12	−4		
$F_{7/2}D_{5/2}$	6	4.28	1.72		$G_{7/2}D_{5/2}$	−18	−32.67	−33.33	
$G_{7/2}P_{1/2}$	−2	−10			$G_{9/2}S_{1/2}$	6	14		
$G_{7/2}P_{3/2}$	−4	−20	−24		$G_{9/2}D_{3/2}$	12	28	30	
$G_{7/2}F_{5/2}$	−6	−4.28	−1.72		$G_{9/2}D_{5/2}$	18	8.67	3.33	
$G_{7/2}F_{7/2}$	−8	−32.38	−45.20	−42.42	$G_{9/2}G_{7/2}$	24	46.90	57.30	51.40
$GPP_{1/2}$	2	10	18						
$G_{9/2}P_{3/2}$	4	20	6						
$G_{9/2}F_{5/2}$	6	30	43.02	40.90					
$G_{9/2}F_{7/2}$	8	6.67	3.82	1.52					

expressed in the form

$$A_{l^\pm}^{(I)}=(\lambda\!\!\!^{-}/2i)[\eta_{l^\pm}^{(I)}\exp(2i\delta_{l^\pm}^{(I)})-1]. \quad (12)$$

The absorption parameter $\eta_{l^\pm}^{(I)}$ is restricted:

$$0\leqslant\eta_{l^\pm}^{(I)}\leqslant 1.$$

$\delta_{l^\pm}^{(I)}$ is the phase shift. $\lambda\!\!\!^{-}=\hbar/|\mathbf{k}_i|$.

Thus each $A_{l^\pm}$ is a complex number, and $(1/\lambda\!\!\!^{-})A_{l^\pm}^{(I)}$ is restricted to the interior of a unit circle, with the point $(0,\frac{1}{2}i)$ as center, in the complex plane. All the quantities mentioned in this section depend on the incident momentum $|\mathbf{k}_i|$. Therefore as $|\mathbf{k}_i|$ is changed the point representing each $A_{l^\pm}^{(I)}$ on the Argand diagram moves about inside the unit circle. The object of this experiment is to determine the behavior of the most significant of the $A_{l^\pm}^{(I)}$, in particular to find out which show resonant behavior. The definition of a resonance is not simple; discussions have been given, for example, by Tripp,[10] Dalitz,[11] and Dalitz and Moorhouse.[12] For our purposes it is adequate to say that a state resonates if the corresponding point traces out a recognizable portion of a circle, including the top. If there is not much "background" amplitude the phase shift passes through 90° or 0° near the resonant energy. This is illustrated clearly by Tripp.[10]

The experiments give values for $d\sigma/d\Omega$ and $(\epsilon/P_T)\times d\sigma/d\Omega$. These can be expanded in series of Legendre polynomials:

$$d\sigma/d\Omega=\sum_{n=0}^{n_{max}} C_n^{(-)}P_n(\cos\theta^*), \quad (13)$$

$$(\epsilon/P_T)d\sigma/d\Omega=\sum_{n=0}^{n_{max}-1} D_n^{(-)}\sin\theta^* P_n(\cos\theta^*). \quad (14)$$

[10] Robert D. Tripp, CERN Report No. 65-7 (unpublished).
[11] R. H. Dalitz, *Strange Particles and Strong Interactions* (Oxford University Press, London, 1962), pp. 64 *et seq.*
[12] R. H. Dalitz and R. G. Moorhouse, Phys. Letters **14**, 159 (1965).

The coefficients $C_n^{(-)}$ and $D_n^{(-)}$ can then be expressed in terms of the $A_{l^\pm}^{(I)}$, via f and g. For $\pi^- p$ scattering we can use $A_{l^\pm}^{(-)}=\frac{2}{3}A_{l^\pm}^{(1/2)}+\frac{1}{3}A_{l^\pm}^{(3/2)}$. Thus

$$C_n^{(-)}=\sum_{\alpha\geq\beta} c_{n\alpha\beta}\,\mathrm{Re}(A_\alpha^{(-)*}A^{\beta(-)}), \quad (15)$$

and

$$D_n^{(-)}=\sum_{\alpha>\beta} d_{n\alpha\beta}\,\mathrm{Im}(A_\alpha^{(-)*}A_\beta^{(-)}), \quad (16)$$

where α, β symbolize the individual values of $l\pm$, ordered in a suitable way. Because the forces involved have finite ranges, we expect the sums to contain a

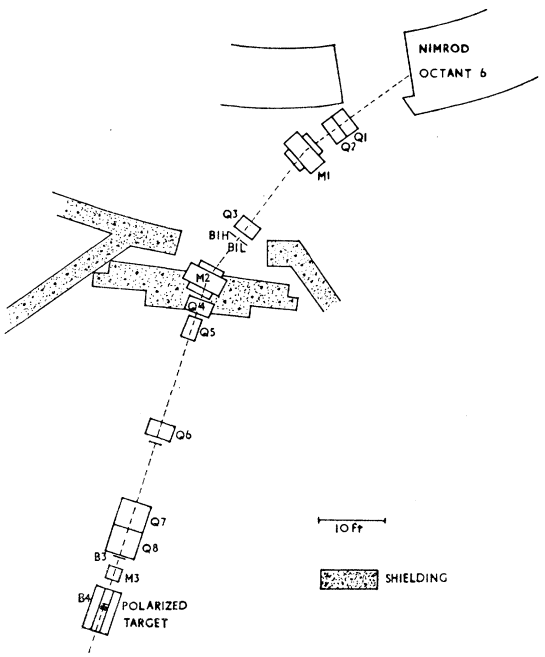

FIG. 1. Beam arrangement.

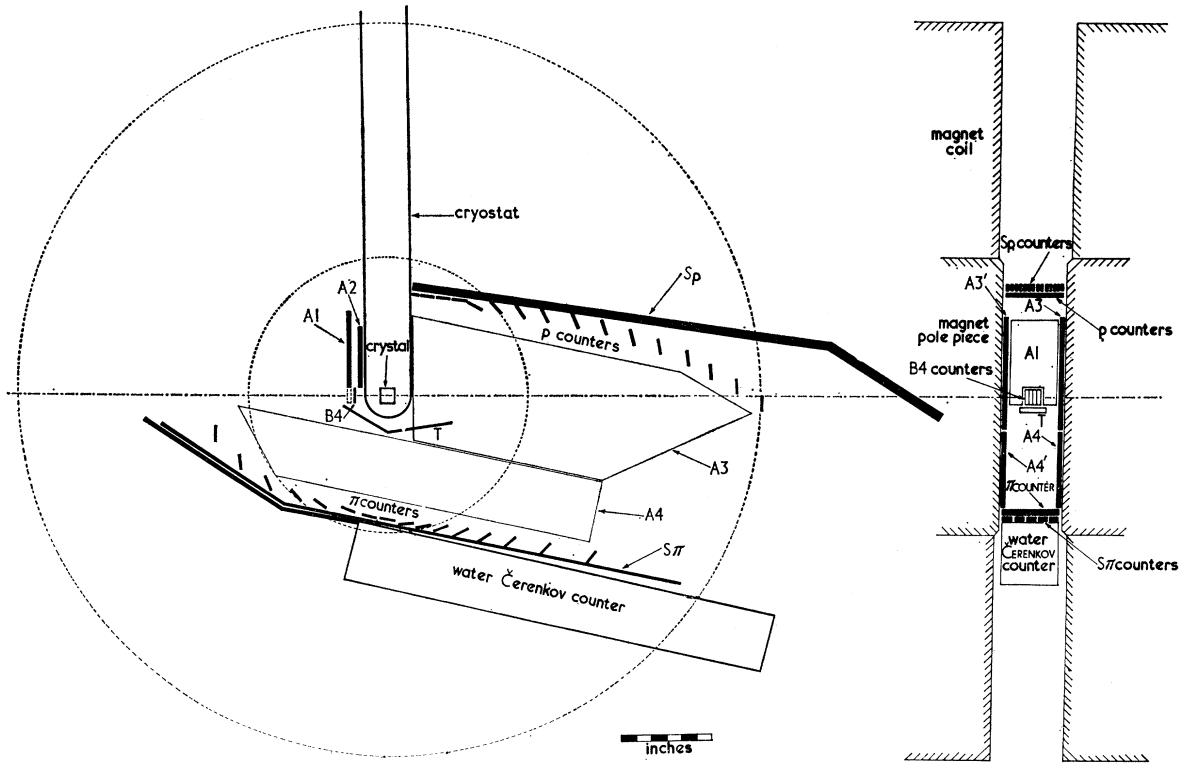

FIG. 2. Arrangement of counters around the polarized target.

finite—and, hopefully, small—numbers of terms. The coefficients $c_{n\alpha\beta}$ and $d_{n\alpha\beta}$ for states with l up to 4 are given in Tables II and III.[13]

III. EXPERIMENTAL ARRANGEMENT

The layout of the beam is shown in Fig. 1. Pions were produced at 26° from an internal target at the end of magnet octant 6 in Nimrod. This target was 2 in. long and was made of tungsten alloy. A quadrupole doublet Q1 Q2 focussed the beam at the center of the horizontally focussing field lens Q3. The bending magnet M1 provided momentum dispersion at the focus at Q3. The beam was deflected again by a magnet M2 and focussed onto the polarized proton target by quadrupoles Q4, Q5, Q6, Q7, and Q8. The angle of deflection in M2 was arranged to cancel the momentum dispersion due to M1. The purpose of Q4–Q8 was to carry the beam to a convenient position for the target. A small bending magnet M3 deflected the beam in a vertical direction. It was used to steer the beam onto the target, which was at the center of a magnet which caused deflection of the beam in the same plane. The momentum was defined by the angle of deflection in M2, determined by counters at B1 and B2. Two counters (B1L and B1H) were placed side by side at B1, thus defining two different momenta. Each momentum band was 5% wide (full width at half-height) and the two were separated by 5% between centers. The magnet M2 was calibrated by the floating-wire technique.

The target consisted of a 1-in. cube of lanthanum magnesium nitrate; Q7 Q8 finally focused the beam onto it. On account of the small spot size required the beam was strongly convergent at the target, particularly in the horizontal plane. The trajectories of the incident pions were defined in the horizontal plane by two hodoscopes consisting of 3 counters B31, B32, B33 at the exit of Q8 and four counters B41, B42, B43, B44 close to the target. In addition these two hodoscopes defined the part of the target crystal through which individual particles passed.

Figure 2 shows the arrangement of counters for detecting scattering events. The polarized target was at the center of a magnet with a 4-in. gap producing a field of 18.5 kG. All the counters shown in Fig. 2 were placed in the gap of this magnet. The incident beam was deflected downwards by the field. Counters A1, A2, A3, A4, A3′ and A4′ were used in anticoincidence to prevent the recording of events in which particles interacted with supporting material, etc., around the target. A signal from counter T indicated that a scattering event had occurred. Scattered pions were detected in 16 π counters below the beam, each $3\frac{1}{2}$ in. long by 1 in. wide. For forward-going particles pions were distinguished from protons by means of a water Čerenkov counter behind the π counters. Recoil

[13] In Ref. 2 there is a numerical error in the expressions for the $d_{n\alpha\beta}$.

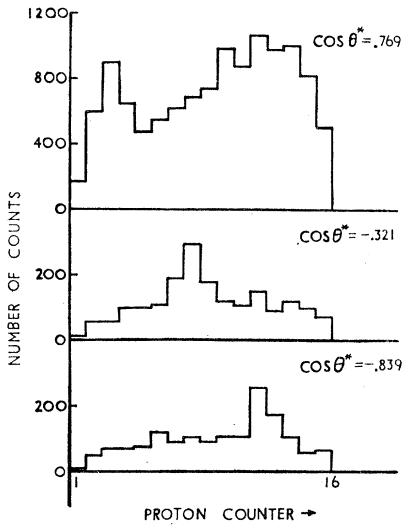

FIG. 3. Typical distributions of counting rate in the p counters. In each distribution a π meson was detected in coincidence at the c.m. angle θ^*. For these examples the momentum was 1030 MeV/c; they were obtained in $1\frac{1}{2}$ h of running, during which time 4×10^8 mesons passed through the target.

protons were detected in an array of 16 p counters above the beam. Because of the compactness of the array of counters and the strong convergence of the beam, the azimuthal angles in a scattered event would not be well defined by the 32 counters described so far. In order to improve the definition of angles, the p array was backed up by 14 long counters Sp1–Sp14; these were arranged to be parallel to the beam axis. The π counters were similarly backed up by 5 strip counters Sπ1–Sπ5. The two sets of strip counters were used in association with the beam hodoscopes B3 and B4 to impose a requirement on the correlation between the azimuthal angles of the two outgoing particles, whereby most noncoplanar events were rejected. Encoded outputs from the p and π counters were connected to the 512-channel storage system of a Laben pulse-height analyzer.

Figure 3 shows some examples of the distribution of counts in the p counters. The peaks due to elastic scattering from the free protons in the target can be seen. Data were taken with the target first polarized in one direction normal to the scattering plane, then with it polarized in the opposite direction. The asymmetry manifested itself as a difference in the heights of corresponding peaks—properly normalized. The background outside the peak region, and also under the peaks, was caused mainly by scattering from the protons bound in the complex nuclei of the target material; the Fermi motion of these protons smeared out the elastic scattering angular correlation. The shape of the background distribution was measured by repeating the experiment with a dummy target containing the same nuclei as the polarized target except for the free protons.

For each beam momentum a function was fitted to the dependence of the background distribution on pion and proton scattering angles. The fitted parameters of this function were then used to estimate the values of the background under the free proton peaks, permitting the appropriate corrections to be made to the asymmetries.

The polarized target was very similar to the one used by Chamberlain *et al.*[7,14] The target consisted of four 1 in.$\times$1 in.$\times\frac{1}{4}$ in. crystals of lanthanum magnesium nitrate, doped with about 1% neodymium. They were immersed in a bath of liquid helium maintained at 1.2°K by pumping the vapor down to a pressure of about 1 mm of mercury. A magnetic field of 18.5 kG in the direction transverse to the pion beam produced polarization of the free protons in this direction. The polarization was enhanced by irradiating the crystal with microwaves of wavelength 4 mm. The average polarization achieved during the experiment was 54%. The degree of polarization was monitored by a nuclear magnetic resonance (NMR) detector coupled to the protons by means of a coil around the target. A fuller description of the polarized target is given by Atkinson *et al.*[15] Calibration runs were made at frequent intervals throughout the experiment by measuring the asymmetry for a beam of protons of 700-MeV kinetic energy and comparing with the polarization measured in proton-proton scattering by Cheng *et al.*[16] The proton beam was obtained by reversing the polarities of all the beam magnets and the polarized target magnet; protons were distinguished from positive pions by the difference in times of flight between the beam counters.

IV. EXPERIMENTAL RESULTS

The physically significant quantity is the asymmetry ϵ divided by the average target polarization P_T. ϵ/P_T is plotted against pion c.m. scattering angle in Fig. 4.[17] For the data at 875, 925, 975, 1030, and 1080 MeV/c the momentum bite $\Delta P/P$ was 5%; for 1280, 1440, and 1579 MeV/c the two blocks of data were lumped together giving a momentum bite of 10%. This data was combined with differential-cross-section data from reference[1] to obtain the quantity $(\epsilon/P_T)d\sigma/d\Omega$. This quantity is plotted in Fig. 5. It is amusing to note that even though a small value of $d\sigma/d\Omega$ implies a large error in ϵ/P_T—since the number of scattering events is then relatively small—nevertheless the absolute error on the product is not unduly large. At each momentum the angular distribution of $(\epsilon/P_T)d\sigma/d\Omega$ was expanded in a series of Legendre polynomials

$$(\epsilon/P_T)d\sigma/d\Omega=\sum_{n=0}^{n_{\max}} D_n^{(-)}\sin\theta^* P_n(\cos\theta^*). \quad (17)$$

[14] C. H. Schultz, Lawrence Radiation Laboratory Report No. UCRL 11149 (unpublished).
[15] H. H. Atkinson, B. E. Belcher, B. F. Colyer, and R. Downton, Rutherford Laboratory Report RPP/N/6 (unpublished).
[16] David Cheng (private communication).
[17] The results of this experiment and experiment (1) are available in numerical form in Rutherford Laboratory Report RHEL/M128 (unpublished).

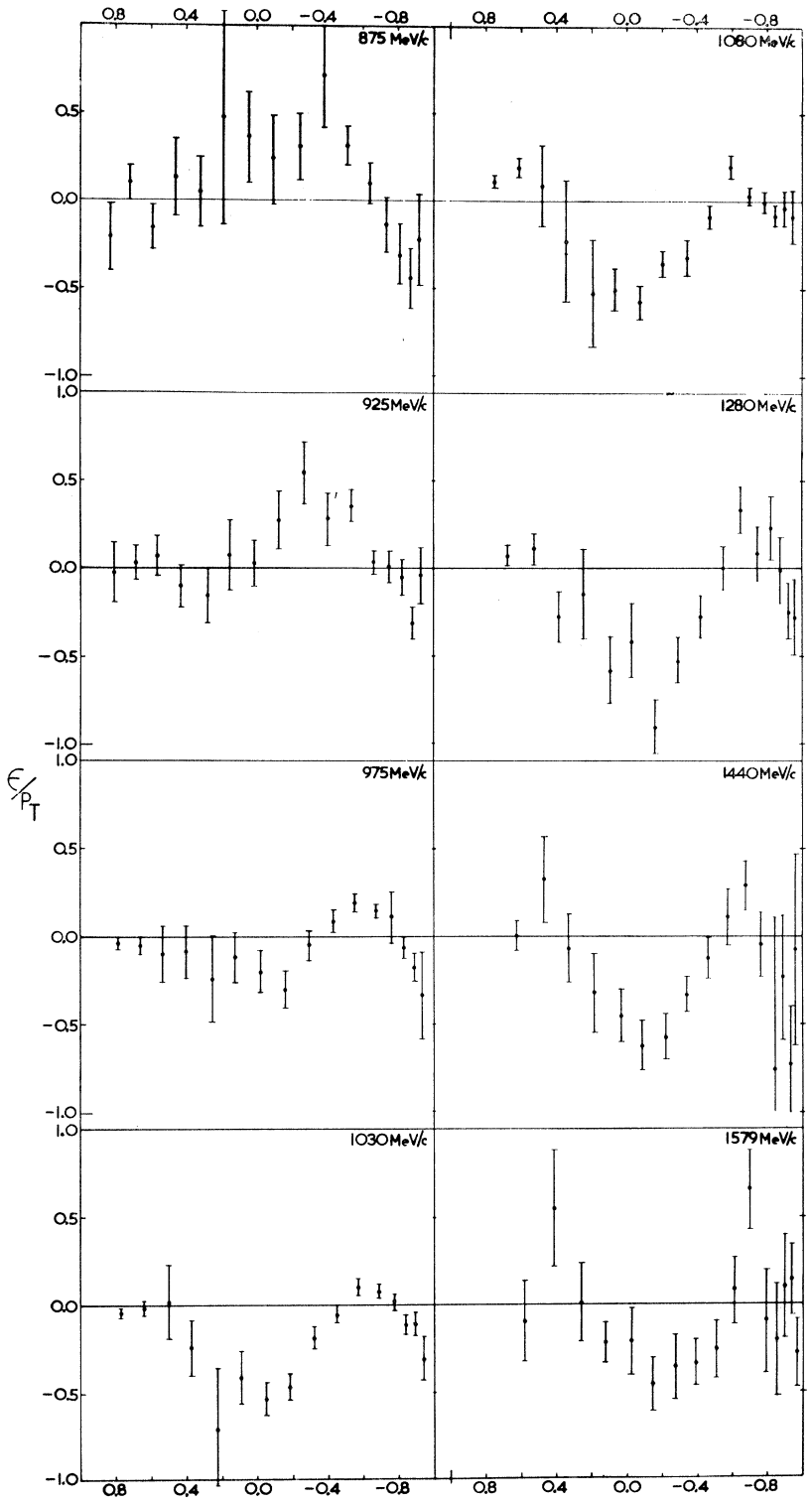

FIG. 4. Normalized asymmetry angular distributions. ϵ is defined to be positive if more mesons scatter to the left when the target is polarized upwards.

Best values for the coefficients $D_n^{(-)}$ were found by the procedure of Ref. 1. The technique described there was used to determine $n_{\max}$ for each momentum. The curves plotted in Fig. 5 are obtained from Eq. (17) using the best-fit values for the $D_n^{(-)}$. The coefficients $D_n^{(-)}$ are plotted against beam momentum in Fig. 6. Fifth-order fits were found to be satisfactory at all the momenta of this experiment. This is in accord with the results of

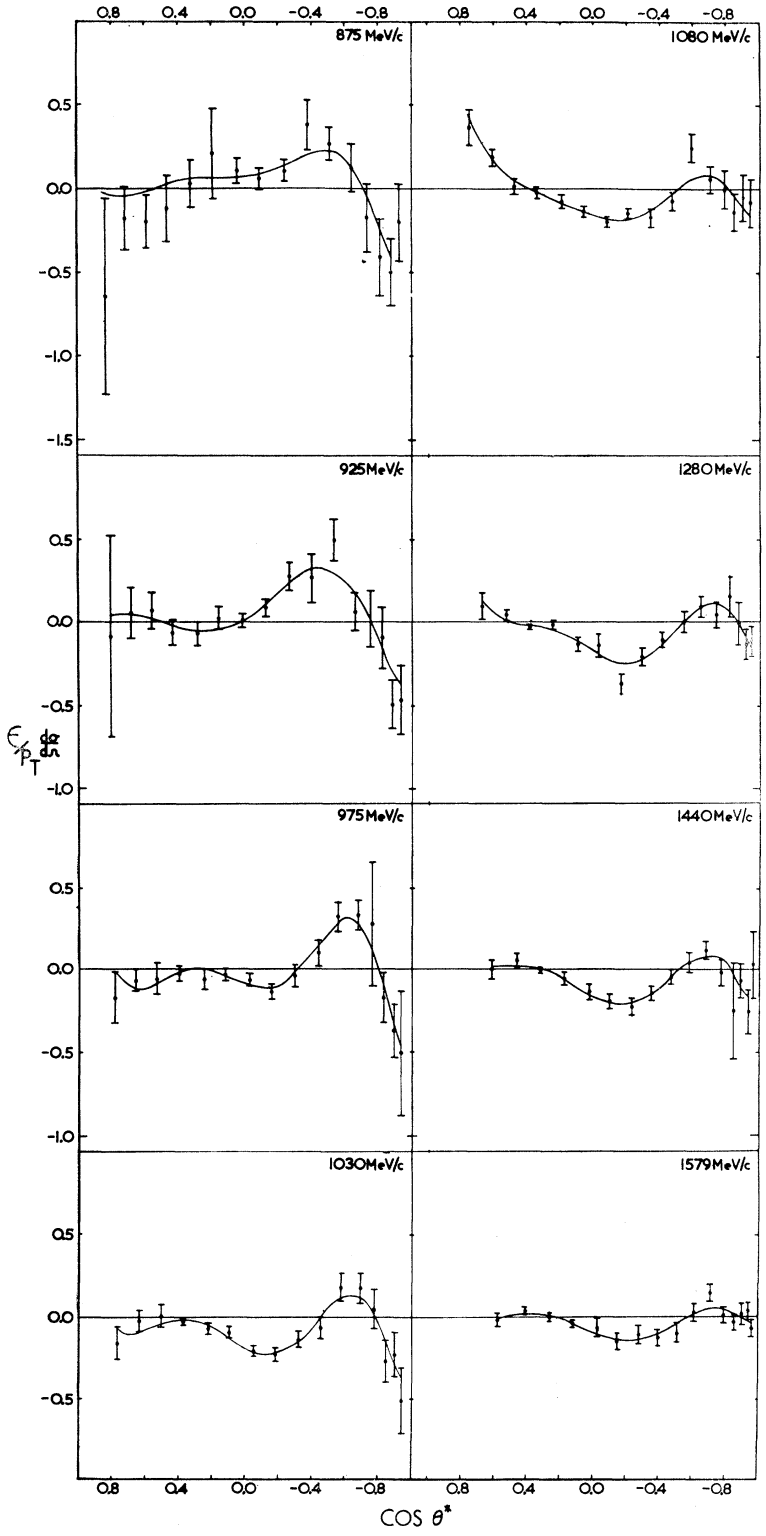

FIG. 5. Angular distributions of $(\epsilon/P_T)d\sigma/d\Omega$. The curves were calculated using the fitting procedure described in the text.

Ref. (1); there the coefficient $C_7^{(-)}$ for the differential-cross-section expansion was found to be small, which implies that $D_6^{(-)}$ must also be small.

V. INTERPRETATION OF RESULTS

In addition to a discussion of the results described in this paper we will also summarize the results of our

experiment on differential cross sections.[1] We will also refer to data on charge-exchange scattering.[18,19]

In principle, differential-cross-section and polarization data should be subjected to a phase-shift analysis; in this type of analysis, values for the $\delta_l^{\pm(I)}$ and the $\eta_l^{\pm(I)}$ are sought which fit the data at each energy. Unfortunately there are insufficient data to give a unique solution at any one energy. Nevertheless, several groups have published unique phase-shift solutions which use the data of this and other experiments; these have been achieved either by introducing theoretical requirements or by choosing those solutions which give a smooth variation with energy.[20–23] While these analyses differ in quantitative details they agree qualitatively. In particular, they agree on the question of which partial-wave amplitudes show resonant behavior in this energy region. Figure 7 shows some of the results obtained by Bareyre *et al.*[23] As can be seen, the amplitudes F_{15}, D_{15}, S_{11}, and S_{31} resonate (the notation is L_{2I2J}, with the usual spectroscopic symbols for L). Since the uniqueness of phase-shift analyses is questionable, we here give independent arguments for some of the assignments. Some of these arguments have already been given.[1,2] The peaks in the π^-p total cross section at 1030 MeV/c and in the π^+p total cross section at 1500 MeV/c have been attributed to resonances $N^*(1688)$ with $I=\frac{1}{2}$ and $N^*(1920)$ with $I=\frac{3}{2}$, respectively.[24]

A. Spin of $N_{1/2}^*(1688)$

The expansion coefficients $C_n^{(-)}$ for the differential cross sections[1] have peaks at about 1030 MeV/c from $n=0$ to $n=5$; $C_6^{(-)}$ is zero very close to this momentum. $C_7^{(-)}$ and $C_8^{(-)}$ are small throughout this momentum range; therefore, states with $J>\frac{7}{2}$ are not strongly excited, and at most one of the two ($F_{7/2}$ and $G_{7/2}$) $J=\frac{7}{2}$ states is excited. We attribute the peaks in the coefficients to a resonance in at least one partial wave. Since there are peaks in $C_5^{(-)}$ and the other odd coefficients, as well as a resonant amplitude, at least one other amplitude—of parity opposite to that of the resonant one—must be strongly excited, possibly also resonant. Let the spins of these two states be J_1 and J_2. The peak in $C_5^{(-)}$ and the absence of a peak in $C_7^{(-)}$

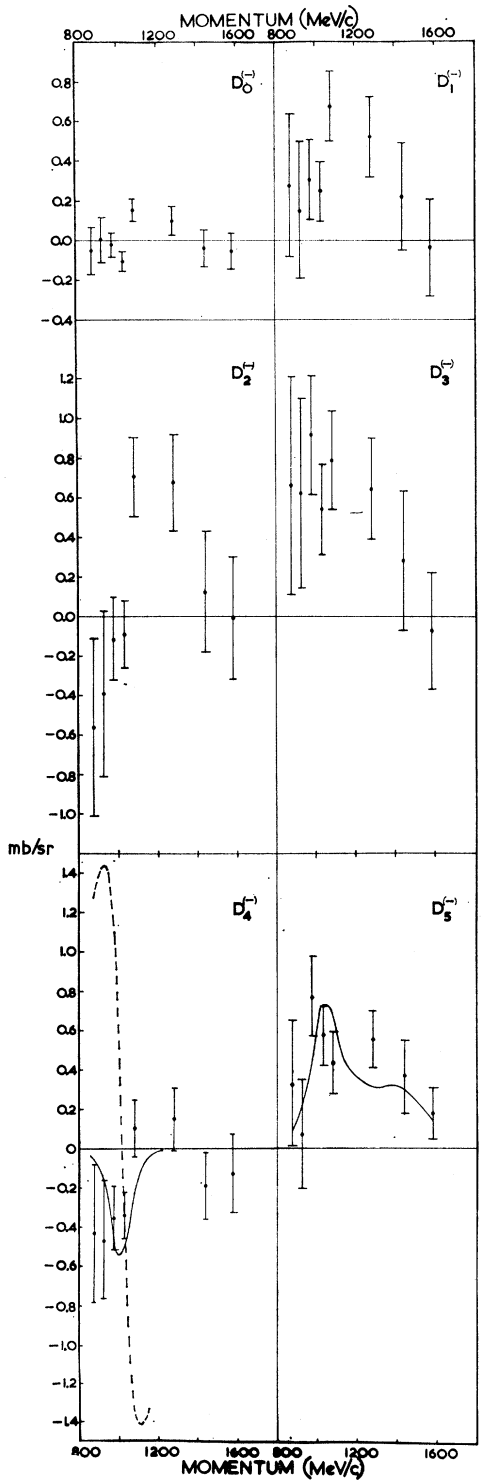

FIG. 6. The coefficients $D_n^{(-)}$ in the expansion

$$(\epsilon/P_T)d\sigma/d\Omega=\sin\theta^*\sum_{n=0}^{5}D_n^{(-)}P_n(\cos\theta^*).$$

The full curves show the behavior to be expected from three resonances $N^*(1920)$ with $I=\frac{3}{2}$, $F_{7/2}$, $N^*(1682)$ with $I=\frac{1}{2}$, $F_{5/2}$, $N^*(1674)$ with $I=\frac{1}{2}$, $D_{5/2}$. The dashed curve for $D_4^{(-)}$ is the behavior expected with no $D_{5/2}$ resonance.

[18] Charles B. Chiu, thesis, University of California, Lawrence Radiation Laboratory Report No. UCRL 16209, 1965 (unpublished); W. Bruce Richards, thesis, University of California, Lawrence Radiation Laboratory report No. UCRL 16195, 1965 (unpublished); C. B. Chiu, R. D. Eandi, A. C. Helmholz, R. W. Kenney, B. J. Moyer, J. A. Doirier, W. B. Richards, R. J. Cence, V. Z. Peterson, N. K. Sehgal, and V. J. Stenger, Phys. Rev. **156**, 1415 (1967).

[19] F. Bulos *et al.*, Phys. Rev. Letters **13**, 558 (1964).

[20] L. D. Roper, Phys. Rev. Letters **12**, 340 (1964).

[21] P. Auvil, A. Donnachie, A. T. Lea, and C. Lovelace, Phys. Letters **12**, 76 (1964).

[22] B. H. Bransden, P. J. O'Donnell, and R. G. Moorhouse, Phys. Letters **11**, 339 (1964).

[23] P. Bareyre, C. Bricman, A. V. Stirling, and G. Villet, Phys. Letters **18**, 342 (1965).

[24] J. A. Helland, T. J. Devlin, D. E. Hagge, M. J. Longo, B. J. Moyer, and C. D. Wood, Phys. Rev. Letters **10**, 27 (1963).

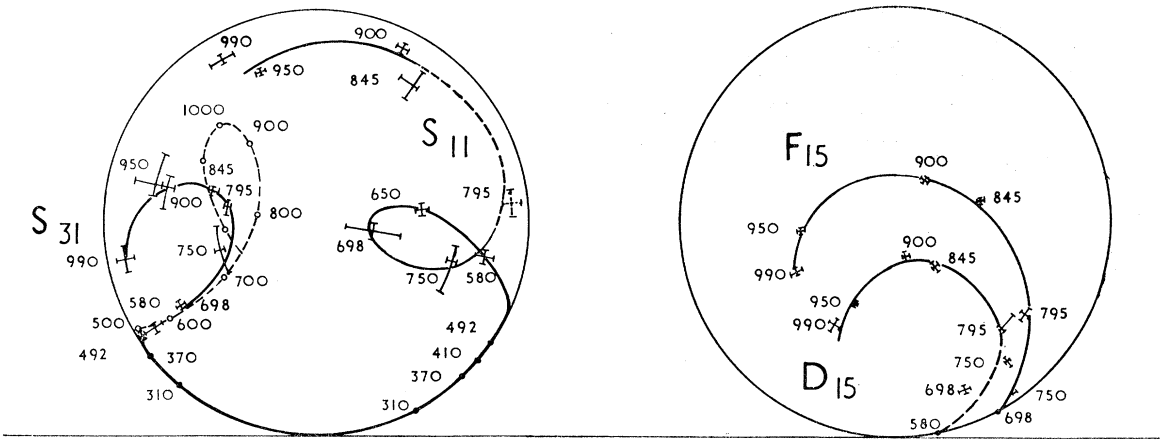

FIG. 7. Some of the results of the phase-shift analysis of Bareyre *et al.* (Ref. 20), which used the results of this and other experiments.

shows that $J_1+J_2\leq 6$. If a state with $J_1=\frac{7}{2}$ resonates there should be a peak in $C_6^{(-)}$, 0.75 times the height of the peak in $C_1^{(-)}$. This could only be avoided by introducing a real nonresonant component in the J_1 amplitude and a third amplitude with $J_3=\frac{5}{2}$ with a suitable real part. Also $F_{7/2}D_{3/2}$ or $G_{7/2}P_{3/2}$ interference contributes nothing to $C_1^{(-)}$, whereas there is a peak in this coefficient, requiring yet more fortuitously excited amplitudes with just the right properties. Thus $J=\frac{7}{2}$ is most unlikely for the resonant state. A $J_1=\frac{3}{2}$ resonance requires strong excitation of the amplitude with $J_2=\frac{7}{2}$ and the opposite parity to explain $C_5^{(-)}$, together with the $J=\frac{5}{2}$ amplitude of the same parity as the resonance to explain $C_4^{(-)}$ and the other $J=\frac{5}{2}$ to explain $C_1^{(-)}$. Even if the appropriate combination of accidents occurred, this seems to be ruled out by $C_6^{(-)}$ being zero at 1030 MeV/c, where the $J_2=\frac{7}{2}$ amplitude needs to be predominantly imaginary, giving a positive, nonzero, $C_6^{(-)}$. Therefore, there must be a

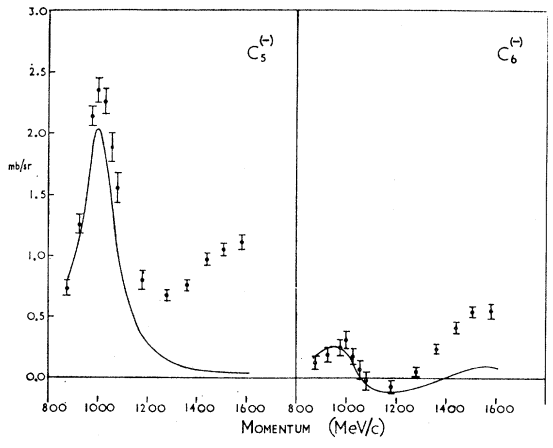

FIG. 8. Coefficients $C_5^{(-)}$ and $C_6^{(-)}$ in $d\sigma/d\Omega=\sum_n C_nP_n(\cos\theta^*)$, measured by Duke *et al.* (Ref. 1). The curves show the behavior expected with the same three resonances as for the full curves of Fig. 6.

$J=\frac{5}{2}$ resonance at this energy. The other $J=\frac{5}{2}$ state must be strong; the energy dependence of the peaks (symmetrical about the resonance energy) requires this state to be either purely imaginary in the neighborhood of the resonance, or else resonant at about the same energy. This is discussed further in Sec. VC. From the sign and magnitude of the coefficient $C_5^{(0)}$ for charge-exchange scattering ($\pi^-p\rightarrow\pi^0n$),[18,19] as compared with $C_5^{(-)}$, it follows that both the $J=\frac{5}{2}$ amplitudes have $I=\frac{1}{2}$. In addition to these amplitudes it is necessary to introduce a $J=\frac{3}{2}$ amplitude to explain the large magnitude of $C_3^{(-)}$.

B. Spin of $N_{3/2}^*(1920)$

In the mass region of 1920 MeV/c^2 (momentum 1500 MeV/c) there are peaks in all the coefficients $C_n^{(+)}$ up to $C_6^{(+)}$; $C_7^{(+)}$ and all higher coefficients are very small.[1] Again it follows that at most one $J=\frac{7}{2}$ state is excited, and no states with higher J are appreciable. The peak in $C_6^{(+)}$ could be due to either (i) a $J=\frac{7}{2}$ resonance, or (ii) a $J=\frac{5}{2}$ resonance interfering with a nonresonant $J=\frac{7}{2}$ amplitude of the same parity. For case (ii) it is necessary to postulate—as well as the $J=\frac{7}{2}$ amplitude—excitation of the other $J=\frac{5}{2}$ state (to explain $C_5^{(+)}$) and also a certain amount of $J=\frac{3}{2}$ and $J=\frac{1}{2}$ to explain the actual magnitudes of $C_3^{(+)}$ and $C_1^{(+)}$. The minimum amounts required for these states already imply a value for $C_1^{(+)}=\sum(J+\frac{1}{2})|A_J|^2$ much larger than is observed. Therefore $J=\frac{7}{2}$ for $N_{3/2}^*(1920)$. Nevertheless, it is interesting to note that the actual magnitudes of the coefficients require $J=\frac{5}{2}$ states of both parities to be nonzero; $C_6^{(+)}$ is actually dominated by the interference term ($F_{7/2}F_{5/2}$ or $G_{7/2}D_{5/2}$) due to its large coefficient. Assuming an $F_{7/2}$ resonance, it is probable that the $D_{5/2}$, $I=\frac{3}{2}$ and $F_{5/2}$, $I=\frac{3}{2}$ amplitudes are predominantly imaginary and the $D_{3/2}$, $I=\frac{3}{2}$ has a large negative real component (from the shape of $C_5^{(+)}$, compared with those of $C_3^{(+)}$ and $C_1^{(+)}$).

C. Parities of $N_{1/2}^*(1688)$ and $N_{3/2}^*(1920)$

$\pi^- p$ scattering has contributions from both $I=\frac{1}{2}$ and $I=\frac{3}{2}$ states. We have seen in Secs. VA and B that there must be resonances with $J=\frac{5}{2}$, $I=\frac{1}{2}$ and $J=\frac{7}{2}$, $I=\frac{3}{2}$ at 1030 and 1500 MeV/c, respectively. Therefore, in $\pi^- p$ scattering there should be energy-dependent interference effects between these momenta. If the two resonances have the same parity then effects should be observed in $C_6^{(-)}$ and $D_5^{(-)}$; if they have opposite parities the highest coefficients affected are $C_5^{(-)}$ and $D_3^{(-)}$. The behavior to be expected for these coefficients can be predicted. Around 1030 MeV/c the $J=\frac{7}{2}$ amplitude is well below resonance; it should be predominantly real and positive in this region. From Tables II and III we see that

$$C_6=3.03|F_{7/2}|^2+18.18\ \mathrm{Re}(F_{7/2}^*F_{5/2})+3.03|G_{7/2}|^2 +18.18\ \mathrm{Re}(G_{7/2}^*D_{5/2}),$$

$$D_5=33.33\ \mathrm{Im}(F_{7/2}^*F_{5/2}-G_{7/2}^*D_{5/2}).$$

(Isotopic spin factors are included in the amplitudes.) At the resonant energy for the $J=\frac{5}{2}$ state the real part of this amplitude passes through zero from positive to negative. If it has the same parity as the $J=\frac{7}{2}$ resonance then $C_6^{(-)}$ should show the same behavior (the small $|F_{7/2}|^2$ or $|G_{7/2}|^2$ term will merely shift the zero point slightly). In fact, $C_6^{(-)}$ does behave in this way. Between 1030 and 1500 MeV/c the charge-exchange coefficient $C_6^{(0)}$ has the opposite sign to $C_6^{(-)}$; this confirms that $C_6^{(-)}$ is due to the interference of states with different I values, as we are supposing. Since the $J=\frac{5}{2}$ state is purely imaginary at 1030 MeV/c, we can rewrite D_5 as

$$D_5=33.33[(\mathrm{Re}F_{7/2})(\mathrm{Im}F_{5/2})-(\mathrm{Re}G_{7/2})(\mathrm{Im}D_{5/2})].$$

We have remarked that whichever of $\mathrm{Re}(F_{7/2})$ or $\mathrm{Im}(G_{7/2})$ is resonant at 1500 MeV/c is positive at 1030 MeV/c, and the other is negligible. Therefore the large positive value of $D_5^{(-)}$ shows that the $J=\frac{7}{2}$ resonance has positive parity; it is $F_{7/2}$. Also we conclude that the $F_{5/2}$, $I=\frac{1}{2}$ state resonates at 1030 MeV/c.

As mentioned in Sec. VA, the $D_{5/2}$, $I=\frac{1}{2}$ state is either predominantly imaginary and slowly varying or resonant near to 1030 MeV/c. We can decide this by considering the behavior of $D_4^{(-)}$ near 1030 MeV/c. From Table III,

$$D_4=-25.71\ \mathrm{Im}(F_{5/2}^*D_{5/2})+24\ \mathrm{Im}(F_{7/2}^*D_{3/2}) +1.72\ \mathrm{Im}(F_{7/2}^*D_{5/2}).$$

The second term should be small and slowly varying, as neither $F_{7/2}$ nor $D_{3/2}$ resonates near 1030 MeV/c. The small coefficient of the third term renders it negligible. Similarly, the energy-dependent part of C_5 in this region is given by

$$C_5=14.29\ \mathrm{Re}(F_{5/2}^*D_{5/2})+5.71\ \mathrm{Re}(F_{7/2}^*D_{5/2}).$$

In the case of an imaginary $D_{5/2}$ the peak value of C_5 is given by

$$C_5(\mathrm{peak})=14.29(\mathrm{Im}F_{5/2})(\mathrm{Im}D_{5/2}).$$

Thus a value for $\mathrm{Im}(D_{5/2})$ can be estimated. Then we calculate $D_4^{(-)}=25.71\ (\mathrm{Re}F_{5/2})(\mathrm{Im}D_{5/2})$. The prediction for this case is plotted as a dashed curve on Fig. 5; it is clearly incorrect. In fact, $D_4^{(-)}$ is much smaller than the prediction. If the $D_{5/2}$ amplitude were to resonate at exactly the same energy as the $F_{5/2}$ does then the resultant polarization would be zero. To explain the observed value of $D_4^{(-)}$ it is necessary to assume that the $D_{5/2}$, $I=\frac{1}{2}$ state resonates slightly below 1030 MeV/c, with the $F_{5/2}$ $I=\frac{1}{2}$ state resonating at that momentum. Figure 8 shows the values of $C_5^{(-)}$ and $C_6^{(-)}$ measured in Ref. 1. The full curves plotted in Figs. 6 and 8 show the expected behavior of the coefficients for the following assumed resonances:

(i) $N_{3/2}^*(1920)$, $\Gamma=170$ MeV, $x=0.41$, $F_{7/2}$;
(ii) $N_{1/2}^*(1682)$, $\Gamma=100$ MeV, $x=0.60$, $F_{5/2}$;
(iii) $N_{1/2}^*(1674)$, $\Gamma=100$ MeV, $x=0.42$, $D_{5/2}$.

Here $x=\Gamma_{el}/\Gamma$. The values for widths and elasticities should not be taken as exact; they are interdependent, they depend on the energy behavior of other amplitudes, and in each case Γ may be energy-dependent. However, they are consistent with the phase-shift analysis of Bareyre *et al.*[23]

ACKNOWLEDGMENTS

We are grateful for the unfailing support of the Nimrod operating crew and of the high-energy physics engineering group. B. Colyer designed the polarized target cryostat. W. M. Evans was responsible for the special electronics. B. Belcher, R. Downton, G. Regan, J. Rice, and G. Morrison took part in the development and operation of the target. P. J. Coleman, N. A. Cumming, L. Lintern, Miss J. E. Robertson, D. C. Thomas, and P. J. Whelan worked long hours on the preparation of the counters and the taking of data. We are grateful to Dr. Bareyre for permission to reproduce some of the results of his group's phase-shift analysis.